Peer-reviewed version available at Materials 2018, 11, 1686; doi:10.3390/ma11091686

Article

Heat-Induced Discoloration of Chromophore Structures in Eucalyptus Lignin

Peng Zhang, Yanxia Wei, Yang Liu, Yao Chen, Jianmin Gao*and Yongming Fan

MOE Key Laboratory of Wooden Material Science and Application, College of Materials Science and Technology, Beijing Forestry University, Beijing 100083, China; rulai9565@hotmail.com (P.Z.); wyx0408@bjfu.edu.cn (Y.W.); nolekobe@sina.com (Y.L.); ychen@bjfu.edu.cn (Y.C.); jmgao@bjfu.edu.cn (J.G.); fanym@bjfu.edu.cn (Y.F.)

* Correspondence: jmgao@bjfu.edu.cn; Tel.: +86-010-6233-7960

Abstract: The color changes corresponding to chromophore structures in lignin caused by exposure of Eucalyptus（Eucalyptus grandis and E. urophylla）to heat were investigated. Eucalyptus wood samples were heated in saturated steam atmospheres for 10 h at 110℃, 130℃, and 150℃. The lignin was isolated before and after heat treatment. The physicochemical properties of the lignin and changes in chromophore structures during heat treatment was evaluated through wet chemical analysis, FTIR, UV-Vis, GPC, XPSand ^{13}C-NMR. The color of the wood became darker and redder with the increase in pressure and temperature. Depolymerization and dehydration reactions occurred via demethoxylation with heat treatment in saturated steam at 110℃ or 130℃. Lignin condensed to form insoluble compounds after heat treatment in saturated steam at 150℃. G units increased and S units decreased through demethylation during heat treatment, as revealed by FTIR and ^{13}C-NMR analysis.

Keywords: heat-induced; wood discoloration; Eucalyptus; lignin; chromophore system.

1. Introduction

Wood is a popular decorative material due to its natural color. Wood products with red and dark hues are especially favored by consumers. Currently, the heat-induced coloring of wood is of greater interest to consumers, due to the global trend of reduced use of solvent-borne finishes, mainly in furniture processing [1]. The addition of no harmful additives and the improvement of color by changing the chromophoric system of wood during heat treatment is an environmentally friendly, stable method [2]. Heat-induced discoloration technology turns light-colored wood to red dark hue, thus providing a potential value for fast-growing wood species [3] and the possibility of reaching new markets where more exotic hardwoods are normally used [4, 5].

The mechanism of heat-induced discoloration of wood is mainly due to chemical changes of cell wall constituents [5-7]. Thermal modifications include decomposition of hemicelluloses [8]; increased crystallinity of cellulose [5]; cleavage of β-O-4 linkages and demethxylation in lignin, resulting in more condensed structures and oxidation products such as quinones [9, 10]. The release of acetic and formic acid by the carbohydrates could catalyze hydrolytic reactions [11, 12], such as oxidation and polymerization of phenolic compounds and lignins. Discoloration during wood heat treatment depends on heating conditions that include heat medium, temperature, moisture content, humidity, and air pressure. The degree of discoloring increases with the temperature, duration time, moisture content, and the presence of oxygen [8]. Thermal treatment under hot air condition ranges from 180 ℃ to 220℃usually causes degradation of hemicellulose and amorphous areas of cellulose [13, 14]. Wikberg (9) using steam as a shielding gas to treat wood samples in 160℃ and 195℃ under normal pressure, achieved the same results as thermal treatment [9]. Chen used saturated steam at 130℃ to induce discoloration, with no change in the structure of cellulose and hemicellulose [2, 15, 16], demonstrating that higher humidity can cause obvious discoloration under saturated steam treated especially at lower temperature, with no effect on polysaccharide components. Although the

Peer-reviewed version available at Materials 2018, 11, 1686; doi:10.3390/ma11091686

saturated steam method effectively induces discoloring, it has received less attention by the wood industry and should be considered. Color changes are presumably more linked to changes in lignin substance than in the carbohydrate fractions [3]. Vacuum drying of Brauns lignin revealed that color change is affected by the variation of Brauns lignin structure [17]. The formation of conjugated structures can also contribute to color formation in the process of lignin degradation under heat treatment [18]. Functional groups in lignin, such as α-carbonyl, biphenyl and ring-conjugated double bonds, are known to absorb UV-light and form chromophores [19]. Quinone and conjunctive carbonyl are the main chromophoric groups, and phenol hydroxyl is the main auxochrome group in wood [20]. Analysis of heat effects in the discoloration mechanism must involve not only wood, but also its isolated lignin.

We here report our study of the effects of steam heat treatment on lignin (especially chromophore structure and content) and its relationship to the discoloration mechanism, and the role of the corresponding changes of the chromophores in the color of wood.

2. Materials and Methods

2.1 Wood samples and thermal modification

Eucalyptus grandis and E. urophylla wood logs were collected from Guangxi Province, southwest China. The wood powder (100 lm-sieved) was air-dried to moisture content 7%-12% before heat treatment. The extractives were removed completely using benzene/alcohol (v/v, 2/1) in a Soxhlet extractor. After extraction, the wood samples were dried for 2 h at 103℃ and then put in a desiccaton until further analysis. The extractive-free wood samples were heated in saturated steam atmosphere for 10 hours at 110℃(0.15MPa), 130℃(0.27MPa) and 150℃(0.49MPa) in an Steam Autoclave (Jiangyin Binjiang, LS-35HD).

2.2 Color measurement

A DF110 spectrophotometer (KONICA MINOLTA CM-2300d) was used to collect the colorimetric data according to the CIEL*a*b* system [21] using 28 standard observer and standard illuminant D65. Five measures were read per sample. The color coordinates lightness L* (varying from 0 for black to 100 for white), a* (varying from negative values for green to positive values for red on the green–red axis) and b* (varying from negative values for blue to positive values for yellow on the blue–yellow axis) were measured. For each test sample, color measurements were performed on 3 points (actually circular areas of about 10 mm diameter, corresponding to the measuring hole) and an average value was calculated. Color differences of the samples before and after heat treatment were calculated based on the following Equations (1)-(4).

$$\Delta L^* = L^*_{\text{heated}} - L^*_{\text{unheated}} \tag{1}$$

$$\Delta a^* = a^*_{\text{heated}} - a^*_{\text{unheated}} \tag{2}$$

$$\Delta b^* = b^*_{\text{heated}} - b^*_{\text{unheated}} \tag{3}$$

$$\Delta E *= \sqrt[2]{\Delta L *^2 + \Delta a *^2 + \Delta b *^2} \tag{4}$$

where ΔL^*, Δa^*, Δb^* and ΔE^* represent the changes in the lightness, green/red coordinate, blue/yellow coordinate, and total color difference, respectively. UV-Visible spectra were recorded at a wavelength range of 200–700 nm on a UV-vis spectrophotometer (Shimadzu CM-2300d, Japan).

2.3 Lignin analysis

Preprints (www.preprints.org) | NOT PEER-REVIEWED | Posted: 16 July 2018 doi:10.20944/preprints201807.0286.v1

Peer-reviewed version available at *Materials* **2018**, *11*, 1686; doi:10.3390/ma11091686

The content of Klason (acid-insoluble) lignin was determined according to ASTM D 1106--96 [22]. The lignin structures before and after heat treatment were determined on dioxane lignin [23, 24]. The dioxane lignin was prepared using the method reported by Evtuguin et al. [25].

Elemental analysis and content of the dioxane lignin was analyzed on a Thermo Scientific Flash 2000 series elemental analyzer. Oxygen content was calculated by subtracting the content of C, H, N, and S from 100% [26, 27].

FTIR (Fourier transform infrared spectroscopy) spectra were recorded in absorbance mode using a PERKIN Elmer Spectrum Gx instrument. The concentration of lignin in a KBr pellet was about 1%. The number of scans was 32, the resolution was 4 cm^{-1}, and the sweep scan range was 400-4000 cm^{-1}. The relative peak height (I′) of carbonyl groups was calculated based on Equation (5).

$$H' = {}^{H}\!/_{H(1507)} \tag{5}$$

where H (1507), H and H′ represent the intensity of 1507cm^{-1}, intensity and relative intensity of carbonyl groups.

The dioxane lignin was acetylated with acetic anhydride/pyridine (1:1, v/v) at 50℃ for 72 h in a sealed container. Ethanol was added, and the volatiles were removed in a vacuum evaporator; the procedure was repeated three times. A gel permeation chromatography (GPC) apparatus with THF (tetrahydrofuran) as eluent at a flow rate of 1.0 mL/min at 25℃ was used to measure the average number of molecular weights (Mn) and molecular weight distributions (PDI), which was calibrated by using linear polystyrene standards [27, 28].

^{13}C CP-MASNMR (Cross Polarization Magic Angle Spinning Nuclear Magnetic Resonance) spectroscopy was recorded using a JNM-ECZ600R NMR spectrometer with a magnetic flux density of 14.09 T. Carbon spectra were acquired with a 4 mm bore probe head. The spinning rate was set to 15 kHz .1024 scans with 3 s delay between successive scans were collected. The length of the contact time was 2 ms, and the spectral width was 37.89 kHz.

X-ray photoelectron spectroscopy analysis was performed on dioxane lignin with a ThermoVG Scientific Sigma Probe using a microfocusing monochromatic AlKaX-ray source at an operating pressure between 10-9 and 10-8 mbar. A high-resolution scan was conducted on the C1S peak from 280 to 300 eV, and the O1S peak from 530 to 535 eV for each sample. Chemical bond analysis of carbon was accomplished by fitting the C1S peak and deconvoluting into four sub peaks for C-C/C=C, C-O, and C=O- groups, with areas represented by C1, C2, C3, respectively. The O1S signals were similarly deconvoluted into two sub peaks for C=O and C-O groups and represented by O1 and O2, respectively. The ratio of C3/C2 and O1/ O2 was calculated [29].

3. Results

3.1. Heat treatment effects on color parameters of wood samples

A summary of CIE Lab color data (L*, a*, and b* average values and calculated color differences ΔE) for the extract-free treated samples are presented in Figure 1. All samples underwent an obvious color change that was perceived visually as darkening and reddening. This demonstrated that saturated steam heat treatment was an effective induced discoloration method. The ΔE value indicated the degree of color change that was elevated dramatically with increasing temperature and pressure, similar to superheated steam conditions [30, 31], which implied that more components absorbing visible light are formed during this process [15]. L*, which was the most sensitive parameter, decreased 20% in each treatment. The parameter a* value, which caused the samples to redden, increased along with the severity of the heat condition and quickly achieved the maximum value, then rose slightly. It is usually implied that the formation of condensation products and oxidation products, such as the quinone-like substances, absorb the complementary light of reddish color in the visible spectrum [2]. The parameter b* value decreased after heating and varied below 20. The gradually higher yellowness after heat treatment could be partly caused by formation of oxygen-containing groups such as carbonyl, carboxyl and hydroperoxide groups, which are mostly pale-yellow substances [12].

Peer-reviewed version available at *Materials* **2018**, *11*, 1686; doi:10.3390/ma11091686

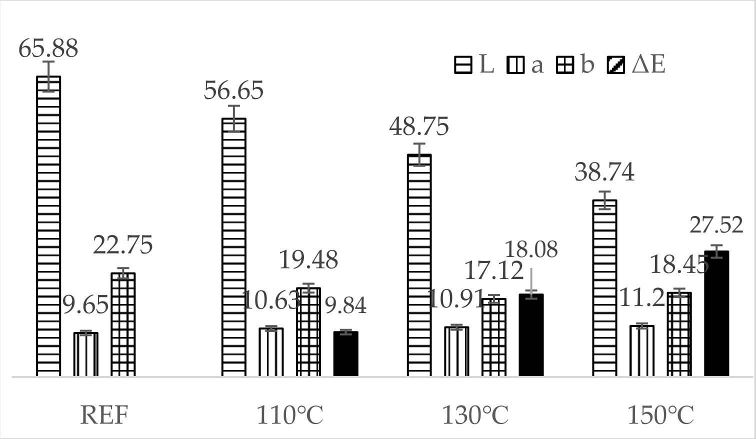

Figure 1. Comparative color parament analyses under saturated steam

Light absorption coefficient spectra can be used to identify qualitative increases in the chromophoric and leucochromophoric structures [32]. UV–Vis diffuse reflectance spectra obtained from the extract-free samples heated at various conditions are shown in Figure 2. The absorptions by all samples obviously increased after heat treatment, which indicated that chromophoric reactions occurred and intensified during steam heat treatment. The color variation can be characterized directly by the reflections in the visible region (380--780 nm). The absorbance in visible region of the sample heat treated at 110℃ increased compared to the reference curve; The absorbance was stronger when the sample heat treated at 130℃; The increase in absorbance in the region of 380--550 was vigorously when heat treated at 150℃, which corresponds to the color parameter changes.

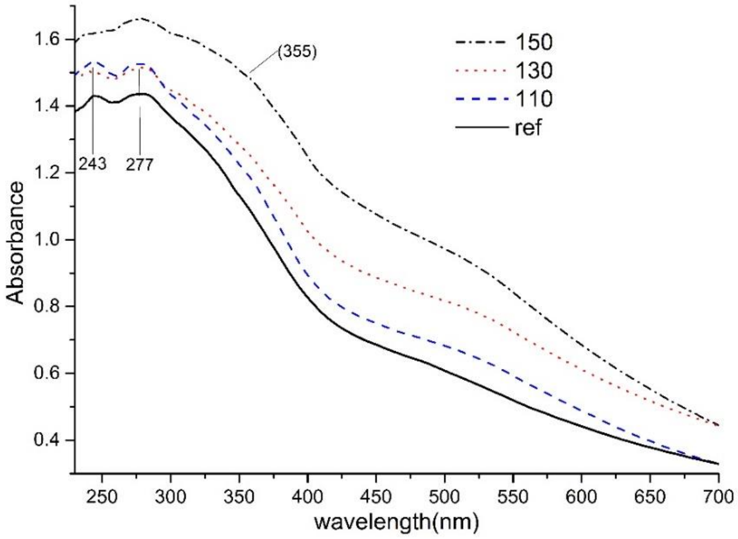

Figure 2. UV spectrum of wood flours treated in saturated steam

For further explanation of discoloration, reflections in the UV region were evaluated. Two peaks (244 nm and 277 nm) intensified with the severity of heat condition. The peak at 244 nm belongs to B band absorbance that represents the benzene ring vibration of aromatic compounds. The peak appearing near 277 nm belongs to the R band absorption, which was the chromophore vibration. In the case of lignin, they are nonconjugated phenolic groups and unsaturated Cα, Cβ bond and β-C = O structure [33]. Samples treated at 110℃ and 130℃ showed the same absorbance in 244 nm and 277 nm peaks, but different in the visible region, which implies that discoloration at 110℃ and 130 ℃ did not originate from chromophoric reactions. Absorbance of these two peaks increased in the 150℃ curves, demonstrating that vigorous chromophoric reactions occurred in this condition, and explaining the increase in optical absorption and color parameters under the 150℃-saturated steam treatment. The spectrum region in 300-400 nm intensified with increasing temperature; the subtle shoulder at 355 nm was attributed to the conjugated structures, such as double bonds and the conjugated carbonyl group in side chains in lignin. Quinoid structures, which resulted from the oxidation of the aromatic hydroxyl groups of lignin, can also contributed to the absorption in the visible region as the subtle shoulders in 300–400 nm.

3.2. Content and Elemental Composition of Lignins

After wood samples were treated and the color variation was evaluated, the lignins were extracted for further study. For the first step, the content changes of acid-insoluble lignin (Klason lignin) and element changes of dioxane lignin were analyzed (Table 1). The klason lignin content variation showed the same direction with the dioxane lignin, which increased for 110℃ and 130℃ conditions and then decreased nearly to the original level in 150℃ treatments.

This trend to increase has been observed in many heat treatment studies [34-36] and is likely due to demethoxylation. At the same time, the O/C ratio was slightly increased, implying that oxidation reactions occurred in lignin during the heat process. Oxidation reactions possibly coincided with demethylation in the C-3/5 position, therefore leading to depolymerization between lignin structural units.

Table1. Chemical composition of lignin during the heat treatment

T (℃)	Klason lignin (%)	Dioxane lignin (%)							
	content	content	C	H	O	N	S	O/C	H/C
REF	22.66(±0.34)	6.06(±0.41)	57.25	5.75	36.79	0.08	0.131	0.48	1.20
110	24.17(±0.21)	11.24(±1.1)	56.06	5.35	38.29	0.10	0.193	0.51	1.15
130	25.4(±0.52)	12.2(±1.8)	55.43	5.19	38.33	0.17	0.884	0.52	1.12
150	21.18(±0.65)	8.08(±0.13)	59.02	5.77	34.90	0.12	0.195	0.44	1.17

The reduction trend was rarely reported in previous studies. The decreased lignin content and the corresponding O/C ratio under the 150℃ conditions could be explained by polymerization of acid-insoluble lignin, followed by reduction reactions. The decrease of O/C suggested that there was a loss of hydroxyl groups when the dehydration reactions occurred [2], which also led to the decrease of hydrogen and oxygen content. Nitrogen in both samples presumably originated from a small amount of proteins from the wood. The proteins are most likely strongly bound to the lignins [37]. Both lignins contained small amounts of sulfur, possibly due to contamination during the washing step. The 150℃-treated condition can be viewed as a turning point for the different trends in 110℃ and 150℃ conditions.

3.3. GPC analysis of molecular weight and polydispersity index

For in-depth studies of reactions of lignin during heat treatment, average molecular weight (Mw and Mn) and polydispersity index (PDI) was determined by GPC analysis (Table 2). The Mw of reference sample was 7025, which was close to the literature reported value of 7590 of MWL. The molecular weight of lignin had two stages of variation. Groups in the 110℃ and 130℃ conditions can be seen as the first stage in which PDI increased, while Mw decreased 56% and 64%, respectively, as compared to the reference lignin. A part of lignin was degraded, leading to an uneven distribution of molecular weight. The aforementioned decrease in hydroxyl groups in lignin as the temperature increasing was consistent with the decreased molecular weight [38].

Table 2. Average molecular weight and molecular weight distribution

Group	Mw (g/ mol)	Mn (g/ mol)	PDI(Mw/Mn)
ref	7025	3822	1.838

110	3962	1483	2.671
130	4513	1687	2.675
150	8777	4332	2.026

The second stage occurred in the 150℃ group where higher Mw (8777) and polydispersity index (2.026) indicating polymerization in part of the lignin, which led to increased molecular weight. Therefore, the molecular weight distribution tends to become even and PDI decreased almost to the original level in the process, which is in accordance with the lignin analysis.In summary, polymerization and oxidation were the main reactions in the first stage (110℃ and 130℃), whereas depolymerization and reduction were predominant in the second stage when the temperature increased to 150℃.

3.4. FTIR spectra of the lignin

Fourier-transform infrared (FTIR) spectroscopy was used to investigate the changes of functional groups. The FTIR spectra of dioxane lignin was normalized at 1507 cm^{-1} (Figure 3), for the aromatic ring vibration around 1510cm^{-1} was stable during treatment [39].

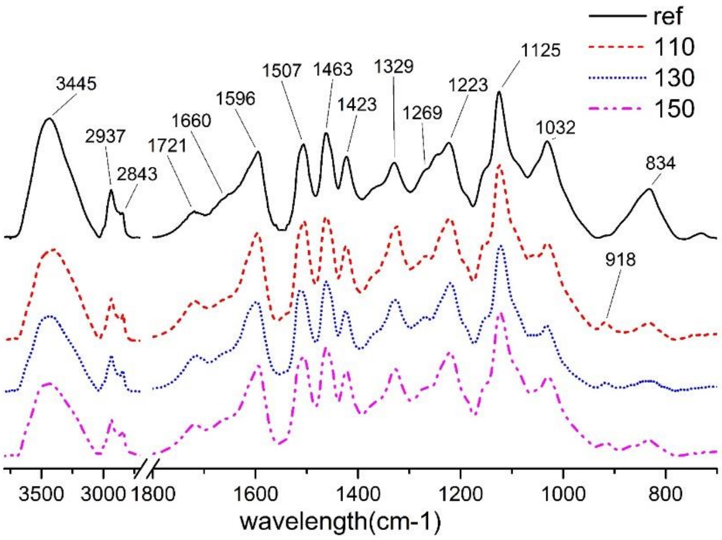

Figure 3. The FTIR spectra of dioxane lignin before and after heat treatment

The decreased intensity of OH stretch vibration at 3445 cm^{-1} implied the reduction of hydroxyl in lignin, such as the C-4 and C-γ positions that were also accompanied with polymerization of lignin. The increased intensity of the CH_2 stretch vibration in 2843 cm^{-1} compared to the reference lignin could be caused by the extended side chain in lignin. The slightly increased vibration of non-conjugated C=O at 1721 cm^{-1} suggests the existence of ester structures and carboxyl groups that will contribute to the darkening of heat-treated samples. The relative peak height (H’) of carbonyl groups, representing the relative content of carbonyl groups, were listed in table 3.

Table 3. Relative peak height (H’) of carbonyl groups in the lignin FTIR spectra

Wave number	**ref**	**110**	**130**	**150**
1660(cm^{-1})	0.44	0.34	0.39	0.37
1721(cm^{-1})	0.29	0.32	0.35	0.31

The content of non-conjugated C=O (1721cm^{-1}) first increased and then decreased, showed the same trend to variation of lignin content and its molecular weight. Wheras, the absorption band at

1660 cm^{-1}, associated with conjugated C=O groups, showed a slight decrease after heat treatment, originating from the depolymerization of lignin. We can conclude that the oxidation reaction led to formation of non-conjugated carbonyl and did not affect conjugated carbonyl groups. After heat treatment, the vibration at 1596 cm^{-1} and 1507 cm^{-1} showed stable aromatic structure during the process. The vibration at 1507 cm^{-1} was especially difficult to change in different heat treatments. The slightly intensified peak at 1329 cm^{-1} implied that the condensation degree of lignin increased during the process. The bands that are associated with guaiacyl units (1269 cm^{-1}, C-O stretch in OCH3; 1125 cm^{-1}; 1032 cm^{-1}, C-H in-plane deformation; 918 cm^{-1}, C-H aromatic out-of-plane deformation) increased after heat treatment, signifying more formation of guaiacyl units which possibly come from the syringyl units through demethxylation. These results are also consistent with bands from syringyl units (1220 cm^{-1}, C-O stretch; 834 cm^{-1}, C-H out-of-plane in position 2 and 6) that decreased after treatment. According to Faix [40], the Eucalyptus dioxane lignin can be classified as a GS4 type whose constituent ratio is H (p-hydroxyphenyl units 0%--5%), G (guaiacyl units 25%--50%), S (syringyl units 45%--70%), and OMe/C900 (135-170). Among various types of lignin, the GS4 type contains the lowest content of G units. In the present study, S units contents decreased because of the demethxylation during the heat treatment

3.5. ^{13}C NMR spectroscopy

^{13}C NMR spectroscopy is a no-destructive technique for obtaining detailed information about lignin structures [27]. The ^{13}C NMR spectrum of dioxane lignin is given in Figure 4.

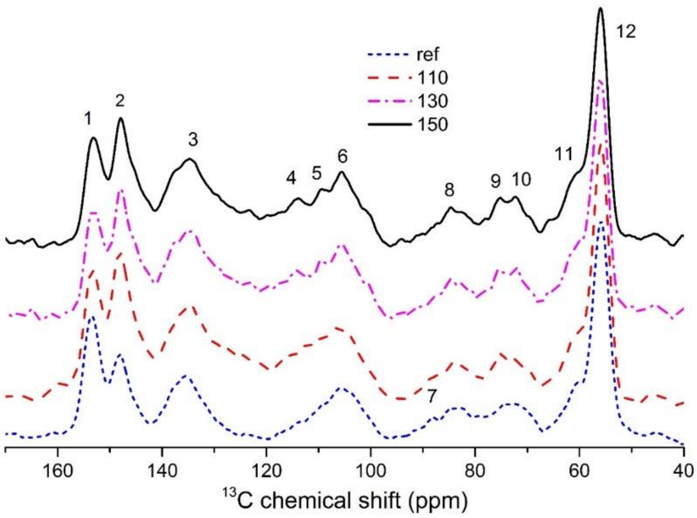

Figure 4. The ^{13}C NMR spectrum of dioxane lignin isolated from treated wood samples

The chemical shifts (ppm), intensity, and assignments as summarized in Table 4, are the results of many previous studies [4, 14, 41, 42]. As can be seen, the lignin fraction is almost absent of typical polysaccharide signals between 57 and 103 ppm (which usually exists in 65, 72, 89, 102, 173 ppm), indicating that the lignin preparation contained only a trace number of associated polysaccharides. The syringyl (S) residues were assigned at 153, 147, 105, and 135 ppm. Guaiacyl (G) residues were verified by signals at 147, 135, and 105 ppm. The p-hydroxyphenyl (H) residues, assigned at 128.1 ppm (C-2/C-6, H) [41], were not detected. These signals revealed that the lignin fraction could be verified as GS lignin, which corresponded to the results obtained by FTIR analysis (Figure 3).The signal intensities were considered to be semiquantitative. The percentage values (%) of carbons are calculated from integrated intensities of signals within each shift range. The integral of the 160-96 ppm region was set as the reference, assuming that it includes six aromatic carbons and 0.12 vinylic carbons. It follows that the integral value (160-102 ppm region）divided by 6.12 is equivalent to one aromatic ring (Ar) [43, 44]. The relative signal intensities were compared in Table 3.

Peer-reviewed version available at *Materials* **2018**, *11*, 1686; doi:10.3390/ma11091686

Table 4. Assignments of the Lignin ^{13}C Signals in the Spectra of the dioxane lignin

	ppm	**Assigment**	**amount (per Ar)**			
			REF	110	130	150
1	153.18	C-3, S etherified	1.71	1.05	1.02	0.91
2	148.05	C-3/5, S non-etherified; C-4, G etherified	1.21	1.27	1.27	1.28
3	134.88	C-1/4, S/G etherified	1.47	1.32	1.35	1.44
4	114.2	C-3/5, H etherified	0.23	0.40	0.39	0.40
5	109.61	C-2, G	0.43	0.42	0.42	0.42
6	105.7	C-5/6, G etherified; C-2/6, S etherified	0.79	0.58	0.57	0.66
7	88.16	C-α, phenylcoumarans	0.21	0.13	0.13	0.12
8	85.02	C-β, β-O-4	0.56	0.33	0.35	0.36
9	75.15	C-a, β-O-4	0.31	0.22	0.24	0.27
10	72.28	C-γ, pinoresinols	0.39	0.22	0.21	0.25
11	60.83	C-γ in β-O-4	0.67	0.45	0.43	0.58
12	56	methoxyl groups OCH3	2.53	1.49	1.41	1.65

Abbreviations: G, guaiacyl unit; S, syringyl unit;

The region between 102 and 162 ppm represents the aromatic part of the lignin that can be further divided into three regions of interest: protonated aromatics (δ123-102 ppm), condensed aromatics (δ140-123 ppm) and oxygenated aromatics (δ 162-140 ppm) [45]. Therefore, a comparison of the integration values of these three regions can provide information relative to the degree of condensation of the lignin fractions. The oxygenated aromatics region shows a stronger intensity at 153 than at 147 ppm in reference lignin, which implies the syringyl-propane units are more involved in ether linkages with other lignin units than the guaiacyl propane structures. The 153 ppm peak intensity reduced and lower than that of 147 ppm after heat treatment show the cleavage degree of the β-O-4 linkages, which results in a decrease in etherified syringyl-propane units [41] and an increase in phenolic structure [2] during the process. The substantial part of the β-O-4 linkages was cleaved, probably due to the steam used in the heat treatment process [46, 47]. This decrease observed for resonance 153 ppm can either be due to the depolymerization of lignins by cleavage of the β-O-4 bonds (which is not the predominant chemical route), or to the demethoxylation of syringyls becoming guaiacyl units. Demethoxylation could explain most of this change since signal 55 ppm, assigned to methoxyl groups, decreases as the temperature increases, which preferentially affects only one methoxyl group of the syringyl units [14]. Demethoxylation of lignin leads to more lignin sites available for reaction. A more condensed lignin structure is achieved as a result.

Thermal modification and steam partially depolymerize wood lignin by hydrolyzing the aryl ether linkages involving C-4 syringyl and guaiacyl units, which leads to the formation of free hydroxyl phenolic groups and α- and β-carbonyl groups. However, no signs of new carbonyl groups (196-193 ppm) are seen in the NMR spectra. Probably at least part of the volatile and water-soluble products, such as depolymerized lignin, were leached out of the wood structure with steam during the modification process and the amount that remained was too low to be detected by solid state NMR [9].

The 135 ppm peak can be classified as a condensed aromatics region which, assigned to C-1 and C-4 of etherified syringyl and guaiacyl units, is stable during steam heat treatment. The condensed aromatic region consists of C-1 carbons plus any ring carbons involved in crosslinking, such as the 5-5 or β-5 substructures. The 105 ppm peak can be classified as protonated aromatics region which rarely change. The occurrence of β-O-aryl ether structure in the dioxane lignin (Fig. 4) is identified with three resonances at 83, 75, and 60 ppm (corresponding to aliphatic carbons bound to oxygen)[48-50], which relate to C-β, C-α, and C-γ in β-O-4 structures, respectively. This magnitude of β-O-aryl ether structures reveals that the treatment with dioxane under the conditions given did not attack the β-aryl ether structure to a significant extent. Also, it is shown that dioxane lignin is a suitable choice for analysis of the present lignin structure. The signals for the γ-methyl, α and β-methylene groups in n-propyl side chains of the lignin fraction should appear in 20 ppm.

3.6. XPS analysis

Figure 5 shows the high-resolution spectra of C1S carbon and O1S oxygen. Table 5 presents the binding energies of C1, C2, C3, O1, O2, plus the C3/C2 and O1/O2 ratios. The relative area of C4, representing carboxylic functionalities, were not detected in the lignin XPS spectrum, which suggests a very low content of carboxylic groups in lignin.

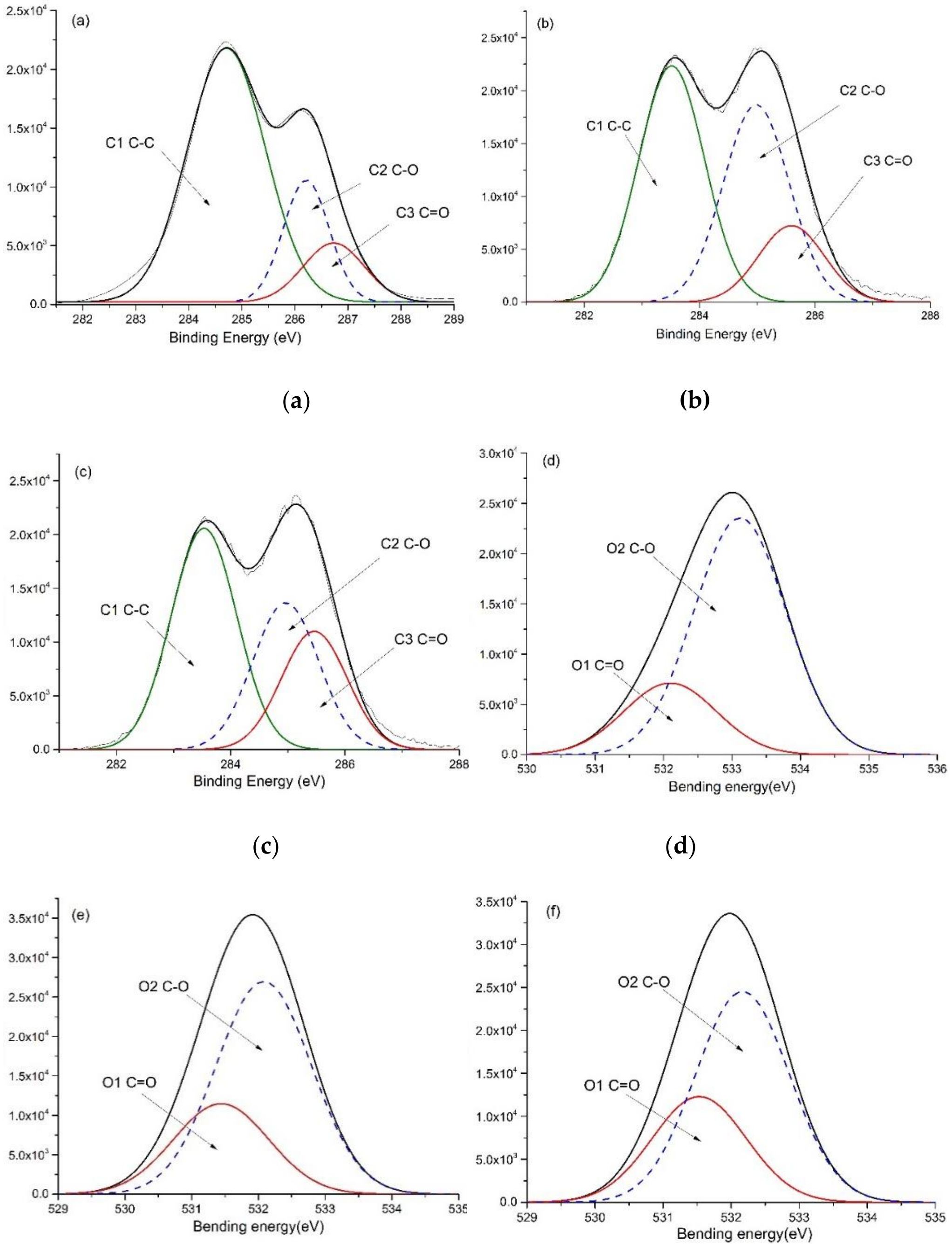

(**a**) (**b**)

(**c**) (**d**)

(**e**) (**f**)

Figure 5. X-ray photoelectron spectroscopy scan of C1S and O1S of lignin isolated from treated wood samples: (**a**) Curve fitting of the C1s peak under 110℃; (**b**) Curve fitting of the C1s peak under 130℃ ; (**c**) Curve fitting of the C1s peak under 150℃; (**d**) Curve fitting of the O1s peak under 110℃; (**e**) Curve fitting of the O1s peak under 130℃; (**f**) Curve fitting of the O1s peak under 150℃

Table.5 Subpeak area fractions of C1S and O1S

Sample description	Relative area of C1s peaks (%)				Relative area of O1s peaks (%)		
	C1 (C-C/C=C) (284.7eV)	C2(C-O) (285.9eV)	C3(C=O) (286.4eV)	C3/C2	O1(C=O) (531.7 eV)	O2(C-O) (532.8 eV)	O1/ O2
ref	57.32	32.84	9.83	0.30	23.20	76.79	0.30
130	46.83	38.20	14.97	0.39	29.83	70.17	0.43
150	45.39	37.40	17.21	0.46	31.80	68.20	0.47

The carbonyl structure produced after heat treatment as demonstrated by increase in the ratios C3/C2 and O1/O2, largely due to increase in C3 and O1 representing non-conjugated C=O group, is confirmed by the intensified peak at 1721 cm^{-1} in FTIR spectra. A similar trend to the lignin content and ratio of O/C appears in C3, that increase for the 110 and 130 conditions but decrease in 150 conditions, imply that various C-O groups affect the PDI, content and O/C ration of lignin. It can be confirmed that the carbonyl structure contributes to the chroma value of a* which increased during the heat treatment. The presence of carbonyl structure and quinone are the reason for a* value [2], which is consistent with unchanged chroma value of a* for different heated samples. The chroma value of b* is influenced by the C-O groups and show the opposite trend to O/C ration of lignin. This can be a more obvious indication for the chromophore variation.

4. Conclusion

The mechanism of steam heat-induced discoloration was investigated via analyzing chromophoric structures in lignin structures. The wood color becomes darker and redder with increasing pressure and temperature; chromophoric reactions in lignin intensify with the severity of conditions. Non-conjugated carbonyl groups and unsaturated Cα, Cβ bond, and β-C =O structure increase in the heat process. Under 110℃ and 130℃ steam heat treatment, depolymerization in lignin forms via demethoxylation. In 150℃ steam treatment, there is a conversion of condensed and dehydration reactions, and the acid-soluble lignin condenses to form insoluble compounds. G units increase and S units decrease through demethylation during the treatment, as confirmed by FTIR and C NMR analysis. Carbonyl structure contribute to the chroma value of a* which increases during the heat treatment. Chroma value of b* is influenced by the C-O groups and show the opposite trend to O/C ratio of lignin.

Author Contributions: P.Z., Y.W. and Y.L. conceived, designed and performed the experiments; Y.C., J.G. analyzed the data; all authors wrote the paper.

Funding: The financial support from the National Natural Science Foundation of China (series project No. 31400498) and the Scientific Research Foundation for the Overseas Returned Scholars, Ministry of Education of China (No. 14JIX-01) is gratefully acknowledged.

Acknowledgments: The MOE Key Laboratory of Wooden Materials Science and Application is gratefully acknowledged.

Conflicts of Interest: The authors declare no conflict of interest. The founding sponsors had no role in the design of the study; in the collection, analyses, or interpretation of data; in the writing of the manuscript, and in the decision to publish the results.

References

1. Fonseca, A. Environmental management in wood processing industries and the european legislation on voc emission control. In 1st International Conference on Environmentally-Compatible Forest Products Oporto, Portugal, 2004; Vol. 1, pp 313-324

2. Chen, Y.; Gao, J.M.; Fan, Y.M.; Tshabalala, M.A.; Stark, N.M. Heat-induced chemical and color changes of extractive-free black locust (robinia pseudoacacia) wood. Bioresources **2012**, 7, 2236-2248,10.15376/biores.7.2.2236-2248.
3. Gonzalez-Pena, M.M.; Hale, M.D.C. Colour in thermally modified wood of beech, norway spruce and scots pine. Part 1: Colour evolution and colour changes. Holzforschung **2009**, 63, 385-393,10.1515/Hf.2009.078.
4. Maunu, S. Nmr studies of wood and wood products. Progress in Nuclear Magnetic Resonance Spectroscopy **2002**, 40, 151-174,10.1016/S0079-6565(01)00041-3.
5. Bekhta, P.; Niemz, P. Effect of high temperature on the change in color, dimensional stability and mechanical properties of spruce wood. Holzforschung **2003**, 57, 539-546, Doi 10.1515/Hf.2003.080.
6. Sundqvist, B. Colour changes and acid formation in wood during heating. doctoral thesis, Luleå tekniska universitet, Sweden, 2004.
7. Kacikova, D.; Kacik, F.; Cabalova, I.; Durkovic, J. Effects of thermal treatment on chemical, mechanical and colour traits in norway spruce wood. Bioresour Technol **2013**, 144, 669-674, 10.1016/j.biortech.2013.06.110.
8. Sivonen, H.; Maunu, S.L.; Sundholm, F.; Jämsä, S.; Viitaniemi, P. Magnetic resonance studies of thermally modified wood. Holzforschung **2002**, 56, 648-654,10.1515/HF.2002.098.
9. Wikberg, H.; Maunu, S.L. Characterisation of thermally modified hard- and softwoods by c-13 cpmas nmr. Carbohydrate Polymers **2004**, 58, 461-466, 10.1016/j.carbpol.2004.08.008.
10. Tjeerdsma, B.; Boonstra, M.; Pizzi, A.; Tekely, P.; Militz, H. Characterisation of thermally modified wood: Molecular reasons for wood performance improvement. Holz als Roh-und Werkstoff **1998**, 56, 149,10.1007/s001070050287.
11. Sundqvist, B.; Karlsson, O.; Westermark, U. Determination of formic-acid and acetic acid concentrations formed during hydrothermal treatment of birch wood and its relation to colour, strength and hardness. Wood Science and Technology **2006**, 40, 549-561,10.1007/s00226-006-0071-z.
12. Liu, X.Y.; Timar, M.C.; Varodi, A.M.; Sawyer, G. An investigation of accelerated temperature-induced ageing of four wood species: Colour and ftir. Wood Science and Technology **2017**, 51, 357-378,10.1007/s00226-016-0867-4.
13. Brito, J.O.; Silva, F.G.; Leao, M.M.; Almeida, G. Chemical composition changes in eucalyptus and pinus woods submitted to heat treatment. Bioresour Technol **2008**, 99, 8545-8548, 10.1016/j.biortech.2008.03.069.
14. Melkior, T.; Jacob, S.; Gerbaud, G.; Hediger, S.; Le Pape, L.; Bonnefois, L.; Bardet, M. Nmr analysis of the transformation of wood constituents by torrefaction. Fue**l** **2012**, 92, 271-280, 10.1016/j.fuel.2011.06.042.
15. Chen, Y.; Fan, Y.M.; Gao, J.M.; Li, H.K. Coloring characteristics of in situ lignin during heat treatment. Wood Science and Technology **2012**, 46, 33-40,10.1007/s00226-010-0388-5.
16. Chen, Y.; Tshabalala, M.A.; Gao, J.; Stark, N.M.; Fan, Y. Color and surface chemistry changes of extracted wood flour after heating at 120 °c. Wood Science and Technology **2013**, 48, 137-150,10.1007/s00226-013-0582-3.
17. Hiltunen, E.; Alvila, L.; Pakkanen, T.T. Characterization of brauns’ lignin from fresh and vacuum-dried birch (betula pendula) wood. Wood science and technology **2006**, 40, 575,10.1007/s00226-006-0072-y.
18. Windeisen, E.; Wegener, G. Behaviour of lignin during thermal treatments of wood. Industrial Crops and Products **2008**, 27, 157-162, 10.1016/j.indcrop.2007.07.015.
19. Sandoval-Torres, S.; Jomaa, W.; Marc, F.; Puiggali, J.-R. Colour alteration and chemistry changes in oak wood (quercus pedunculata ehrh) during plain vacuum drying. Wood Science and Technology **2012**, 46, 177-191,10.1007/s00226-010-0381-z.
20. Sandoval-Torres, S.; Jomaa, W.; Marc, F.; Puiggali, J.-R. Causes of color changes in wood during drying. Forestry Studies in China **2010**, 12, 167-175,10.1007/s11632-010-0404-8.
21. Mononen, K.; Alvila, L.; Pakkanen, T.T. Ciel* a* b* measurements to determine the role of felling season, log storage and kiln drying on coloration of silver birch wood. Scandinavian journal of forest research **2002**, 17, 179-191,10.1080/028275802753626827.
22. ASTM. Astm d1106-96 standard test method for acid-insoluble lignin in wood. 2013;
23. Adler, E. Lignin chemistry—past, present and future. Wood science and technology 1977, 11, 169-218,10.1007/BF00365615.
24. Lin, S.Y.; Dence, C.W. Methods in lignin chemistry. Springer Science & Business Media: **2012**,3642740650.
25. Evtuguin, D.V.; Neto, C.P.; Silva, A.M.; Domingues, P.M.; Amado, F.M.; Robert, D.; Faix, O. Comprehensive study on the chemical structure of dioxane lignin from plantation eucalyptus globulus wood. J Agric Food Chem **2001**, 49, 4252-4261,10.1021/jf010315d.

Peer-reviewed version available at *Materials* **2018**, *11*, 1686; doi:10.3390/ma11091686

26. Gabov, K.; Gosselink, R.J.; Smeds, A.I.; Fardim, P. Characterization of lignin extracted from birch wood by a modified hydrotropic process. J Agric Food Chem **2014**, 62, 10759-10767,10.1021/jf5037728.
27. Hu, Z.J.; Du, X.Y.; Liu, J.; Chang, H.M.; Jameel, H. Structural characterization of pine kraft lignin: Biochoice lignin vs indulin at. Journal of Wood Chemistry and Technology **2016**, 36, 432-446,10.1080/02773813.2016.1214732.
28. Wang, J.; Wu, B.; Li, S.; He, Y. Nir light and enzyme dual stimuli-responsive amphiphilic diblock copolymer assemblies. Journal of Polymer Science Part A: Polymer Chemistry **2017**, 55, 2450-2457,10.1002/pola.28632.
29. Chen, Y.; Fan, Y.; Gao, J.; Tshabalala, M.A.; Stark, N.M. Spectroscopic analysis of the role of extractives on heat-induced discoloration of black locust (robinia pseudoacacia). Wood Material Science & Engineering **2012**, 7, 209-216,10.1080/17480272.2012.669407.
30. Charrier, B.; Haluk, J.; Janin, G. Prevention of brown discoloration in european oakwood occurring during kiln drying by a vacuum process: Colorimetric comparative study with a traditional process. Holz als Roh- und Werkstoff **1992**, 50, 433-437,10.1007/BF02662781.
31. Burtin, P.; Jay-Allemand, C.; Charpentier, J.-P.; Janin, G. Modifications of hybrid walnut (juglans nigra 23 x juglans regia) wood colour and phenolic composition under various steaming conditions. Holzforschung **2000**, 54, 33-38,10.1515/HF.2000.006.
32. Johansson, M. Formation of chromophores and leucochromophores during manufacturing of mechanical pulp. Licentiate Thesis, Royal Institute of Technology, u, Stockholm, 2000.
33. Sun, J.X.; Sun, X.F.; Sun, R.C.; Fowler, P.; Baird, M.S. Inhomogeneities in the chemical structure of sugarcane bagasse lignin. J Agric Food Chem **2003**, 51, 6719-6725,10.1021/jf034633j.
34. Nguila Inari, G.; Petrissans, M.; Gerardin, P. Chemical reactivity of heat-treated wood. Wood Science and Technology **2006**, 41, 157-168,10.1007/s00226-006-0092-7.
35. Rousset, P.; Lapierre, C.; Pollet, B.; Quirino, W.; Perre, P. Effect of severe thermal treatment on spruce and beech wood lignins. Annals of Forest Science **2009**, 66, 1, 10.1051/forest/2008078.
36. Park, J.; Meng, J.J.; Lim, K.H.; Rojas, O.J.; Park, S. Transformation of lignocellulosic biomass during torrefaction. Journal of Analytical and Applied Pyrolysis **2013**, 100, 199-206, 10.1016/j.jaap.2012.12.024.
37. Gosselink, R.J.A.; Abacherli, A.; Semke, H.; Malherbe, R.; Kauper, P.; Nadif, A.; van Dam, J.E.G. Analytical protocols for characterisation of sulphur-free lignin. Industrial Crops and Products **2004**, 19, 271-281, 10.1016/j.indcrop.2003.10.008.
38. Kim, J.Y.; Hwang, H.; Oh, S.; Kim, Y.S.; Kim, U.J.; Choi, J.W. Investigation of structural modification and thermal characteristics of lignin after heat treatment. Int J Biol Macromol **2014**, 66, 57-65, 10.1016/j.ijbiomac.2014.02.013.
39. Nakano, J. Chemistry of lignin——basis and application. Translated by gao jie, bao he, li zhongzheng Beijing: Light Industry Press: 1988,7-5019-0286-0.
40. Faix, O. Classification of lignins from different botanical origins by ft-ir spectroscopy. Holzforschung 1991,10.1515/hfsg.**1991**.45. s1.21.
41. She, D.A.; Xu, F.; Geng, Z.C.; Sun, R.C.; Jones, G.L.; Baird, M.S. Physicochemical characterization of extracted lignin from sweet sorghum stem. Industrial Crops and Products **2010**, 32, 21-28, 10.1016/j.indcrop.2010.02.008.
42. Nimz, H.; Robert, D.; Faix, O.; Nemr, M. Carbon-13 nmr spectra of lignins, 8. Structural differences between lignins of hardwoods, softwoods, grasses and compression wood. Holzforschung-International Journal of the Biology, Chemistry, Physics and Technology of Wood **1981**, 35, 16-26
43. Capanema, E.A.; Balakshin, M.Y.; Kadla, J.F. A comprehensive approach for quantitative lignin characterization by nmr spectroscopy. J Agric Food Chem **2004**, 52, 1850-1860,10.1021/jf035282b.
44. Chen, C.-L. Characterization of milled wood lignins and dehydrogenative polymerisates from monolignols by carbon-13 nmr spectroscopy. ACS Publications: 1998.10.1021/bk-1998-0697.ch018
45. Brosse, N.; El Hage, R.; Chaouch, M.; Petrissans, M.; Dumarcay, S.; Gerardin, P. Investigation of the chemical modifications of beech wood lignin during heat treatment. Polymer Degradation and Stability **2010**, 95, 1721-1726, 10.1016/j.polymdegradstab.2010.05.018.
46. Haw, J.F.; Schultz, T.P. Carbon-13 cp/mas nmr and ft-ir study of low-temperature lignin pyrolysis. Holzforschung-International Journal of the Biology, Chemistry, Physics and Technology of Wood **1985**, 39, 289-296,10.1515/hfsg.1985.39.5.289.

Peer-reviewed version available at *Materials* **2018**, *11*, 1686; doi:10.3390/ma11091686

47. Haw, J.F.; Maciel, G.E.; Biermann, C.J. Carbon-13 nuclear magnetic resonance study of the rapid steam hydrolysis of read oak. Holzforschung-International Journal of the Biology, Chemistry, Physics and Technology of Wood **1984**, 38, 327-331,10.1515/hfsg.1984.38.6.327.
48. Zhang, F.; Lin, J.; Zhao, G. Preparation and characterization of modified soda lignin with polyethylene glycol. Materials (Basel) **2016**, 9, 822,10.3390/ma9100822.
49. Jiang, X.; Liu, J.; Du, X.Y.; Hu, Z.J.; Chang, H.M.; Jameel, H. Phenolation to improve lignin reactivity toward thermosets application. Acs Sustainable Chemistry & Engineering **2018**, 6, 5504-5512,10.1021/acssuschemeng.8b00369.
50. Jiang, X.; Savithri, D.; Du, X.; Pawar, S.N.; Jameel, H.; Chang, H.M.; Zhou, X. Fractionation and characterization of kraft lignin by sequential precipitation with various organic solvents. Acs Sustainable Chemistry & Engineering **2016**, 5,10.1021/acssuschemeng.6b02174.